Thermochimica Acta, 205 (1992) 289–298
Elsevier Science Publishers B.V., Amsterdam

Thermodynamic properties of $NiCr_2O_4$–$NiFe_2O_4$ spinel solid solution

Bong-Hoon Park and Hideaki Suito

Research Institute of Mineral Dressing and Metallurgy, Tohoku University, Katahira, Aoba-ku, Sendai 980 (Japan)

(Received 16 October 1991)

Abstract

The tie lines delineating ion-exchange equilibria between $NiFe_2O_4$–$NiCr_2O_4$ spinel solid solution and Fe_2O_3–Cr_2O_3 corundum solid solution were determined at 900, 1000 and 1200°C by electron microprobe and energy dispersive X-ray analysis of oxide phases, using the flux-growth technique. The activities of the spinel components were calculated from the tie lines, assuming Temkin's ideal mixing in the corundum solid solution. The spinel phase can be expressed by a regular solution with negative deviations from ideality. The Gibbs free energies of mixing for spinel solid solution are discussed in terms of the cation distribution model, based on site preference energies and assuming random mixing on both tetrahedral and octahedral sites.

INTRODUCTION

Spinel phases play an important role in the oxidation of alloys, in the formation of inclusions, and in the refining of metals. There have been extensive studies on the thermodynamic properties of spinel solid solution. Several attempts have been made to characterize the cation distribution in certain spinel systems and to relate the thermodynamic properties to structure information [1–4].

For the determination of tie lines delineating two phases, the present author group [5,6] applied the newly developed experimental technique of using the flux-growth method based on the Ostwald ripening mechanism.

The aim of the present investigation is to provide the information on spinel–corundum phase relations in the NiO–Fe_2O_3–Cr_2O_3 system and to obtain the activities for spinel phases whose data are not available in the literature. Gibbs energies of mixing in spinel solid solution are compared to those obtained from a cation distribution model [2].

Correspondence to: H. Suito, Research Institute of Mineral Dressing and Metallurgy, Tohoku University, Katahira, Aoba-ku, Sendai 980, Japan.

EXPERIMENTAL

The materials used in the present work were α-Fe_2O_3 (Rare metallic, $Fe_2O_3 > 99.99$ wt.%), and reagent grade $Na_2B_4O_7$, Cr_2O_3 and NiO. The average sizes of the α-Fe_2O_3, Cr_2O_3 and NiO crystals, determined by SEM, were 0.1, 1.0 and 1.0 μm, respectively. An excess amount of these fine powders, about 1.5 times greater than the corresponding solubility, was mixed in appropriate proportion with $Na_2O \cdot 2B_2O_3$ flux. Samples (15 g) in a Pt crucible were stirred with a Pt stirrer (10 rad s^{-1}) to homogenize the liquid composition at 900, 1000 and 1200°C under a dry air atmosphere. After maintaining for 2–8 h at the required temperature, the sample was quenched in water. No solid solution phases were confirmed as being precipitated on quenching. The contents of the spinel and corundum components were determined by analyzing each element in the crystal grains, using electron microprobe analysis and energy dispersive X-ray spectrometry rather than chemical analysis, because of the difficulty in separating the two phases. More detailed descriptions of the techniques are given in previous papers [5,6].

RESULTS AND DISCUSSION

The tie line between corundum and spinel phases

A new technique of crystal growth by Ostwald ripening [5,6] used here is briefly described below. The initial Fe_2O_3, NiO and Cr_2O_3 crystals with an average size of 0.1–1.0 μm in a saturated solution of $Na_2O \cdot 2B_2O_3$ flux, were found to grow to a size of 10–20 μm over a period of 2–8 h. The observed growth of the crystals was confirmed as being due to the Ostwald ripening mechanism in which the driving force is the reduction of the total interfacial energy of the larger crystals. More details of this mechanism are discussed elsewhere [5,6]. The corundum and spinel crystals were formed under equilibrium conditions during Ostwald ripening, owing to the low degree of supersaturation with respect to crystal growth.

The experimental results for the equilibrium compositions are summarized in Table 1, and the tie lines delineating the spinel and corundum solid solution at 800, 900 and 1200°C are shown in Fig. 1, which shows that the deviation from stoichiometric spinel composition increases with an increase in temperature, and tends to decrease with increasing nickel content.

Tie lines in the region of Fe_2O_3-poor compositions could not be determined because the Na_2O–Fe_2O_3–Cr_2O_3 solid solution was observed to be formed. The contents of Na and B in both phases were found to be less than 30 ppm (by weight), respectively.

TABLE 1

Tie-line compositions of $Ni_{0.5}CrO_2$–$Ni_{0.5}FeO_2$ and $FeO_{1.5}$–$CrO_{1.5}$ at 900, 1000 and 1200°C

Temp. (°C)	Corundum			Spinel		
	$x_{CrO_{1.5}}$ (mol.%)	$x_{FeO_{1.5}}$ (mol.%)	x_{NiO} (mol.%)	$x_{CrO_{1.5}}$ (mol.%)	$x_{FeO_{1.5}}$ (mol.%)	x_{NiO} (mol.%)
900	0.10	0.90	0	0.04	0.49	0.47
	0.22	0.78	0	0.08	0.44	0.48
	0.36	0.64	0	0.12	0.40	0.48
	0.68	0.32	0	0.21	0.32	0.47
	0.84	0.16	0	0.28	0.24	0.48
1000	0.08	0.92	0	0.03	0.50	0.47
	0.20	0.80	0	0.07	0.46	0.47
	0.31	0.69	0	0.10	0.41	0.49
	0.54	0.45	0.01	0.19	0.33	0.48
	0.68	0.31	0.01	0.22	0.28	0.50
	0.72	0.27	0.01	0.25	0.27	0.48
	0.76	0.23	0.01	0.27	0.25	0.48
1200	0.10	0.90	0	0.07	0.55	0.38
	0.23	0.77	0	0.14	0.47	0.39
	0.39	0.61	0	0.17	0.39	0.44
	0.56	0.41	0.03	0.24	0.33	0.43
	0.68	0.29	0.03	0.27	0.28	0.45

Stoichiometry of spinel solid solution

In the present experimental conditions, ferrous ions are produced, as predicted from previous studies [7–9] concerning the phase equilibria in the ferrite region of the Fe–Ni–O system as a function of temperature and oxygen partial pressure. Therefore, the data points should be plotted in the Fe_2O_3–FeO–Cr_2O_3–NiO quarternary system, not in the ternary system

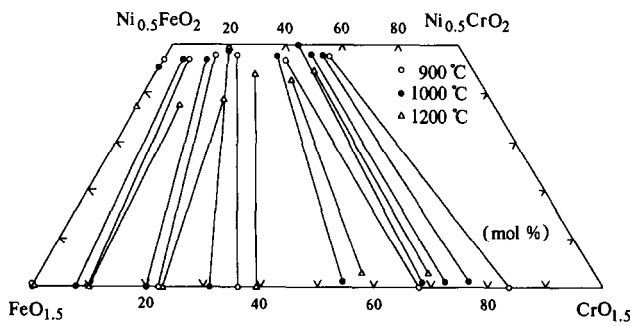

Fig. 1. Phase diagram of the NiO–Fe_2O_3–Cr_2O_3 system, showing tie lines between spinel and corundum phases at 900, 1000 and 1200°C.

shown in Fig. 1. However, because the ferrous content in the spinel solid solutions could not be determined by the present analytical method, the data points are plotted in the Fe_2O_3–Cr_2O_3–NiO ternary system, assuming that the Fe contents determined are equal to those for Fe^{3+} ion. It should be noted therefore, that the standard state for $NiFe_2O_4$ is not the oxygen-saturated phase in equilibrium with Fe_2O_3.

The data points at 900 and 1000°C, having a comparatively small deviation from the stoichiometric spinel composition, were used for the calculation of activities in the spinel phase described below.

Estimation of activities in Fe_2O_3–Cr_2O_3 solid solution

Pelton et al. [10] calculated the excess free energy of mixing of the corundum phase from the equation $G^{ex} = -7500x(1-x)$ J mol^{-1}, after a computer analysis coupling thermodynamic and phase diagram information. However, Petric and Jacob [11] pointed out that their value for G^{ex} had to be corrected because Pelton et al. [10] did not take into consideration the works of Cremer [12], and Snethlage and Klemm [13] regarding activities in the Fe_3O_4–$FeCr_2O_4$ spinel solid solution, but adopted the activity data of Schmahl and Dillenburg [14] which are inconsistent with all other data.

Petric and Jacob [11] measured activities in the Fe_3O_4–$FeCr_2O_4$ spinel solid solution by equilibrating with Pt under controlled CO/CO_2 gas mixtures at 1400°C. Their results agree well with those of Katsura et al. [15], who derived activities of Fe_3O_4 in spinel solid solution at 1227°C. The free energy of mixing in this system obtained by Petric and Jacob [11] is slightly less than those reported by Snethlage and Klemm [13] at 1200°C, but significantly greater than the values given by Schmahl and Dillenburg [14] at 900°C.

Furthermore, Petric and Jacob [11] confirmed the validity of their experimentally determined activities of Fe_3O_4 and $FeCr_2O_4$ in the following two calculations. First, using a modified Gibbs–Duhem equation [16], they derived the activities of spinel components from the tie lines delineating the spinel and corundum solid solutions obtained by Snethlage and Klemm [13] at 1200°C, assuming that the corundum solid solution Fe_2O_3–Cr_2O_3 is an ideal Temkin mixing. These calculated results are in good agreement with those of Petric and Jacob [11] at 1400°C and Katsura et al. [15] at 1223°C. Secondly, Petric and Jacob [11] calculated activities of Fe_3O_4 and $FeCr_2O_4$ from the equilibria $2Fe_3O_4 + 0.5O_2 = 3Fe_2O_3$ and $Cr_2O_3 + Fe_3O_4 = FeCr_2O_4 + Fe_2O_3$, using the Temkin model in corundum phase and the three tie lines obtained at 1300°C by Katsura et al. [15] and Muan [16]. Then they obtained the free energy of mixing in the spinel phase. As a result, the calculated Gibbs energy of mixing was found to be in better agreement with the results of Petric and Jacob [11].

Therefore, it seems that the mixing of the corundum solid solution is ideal according to the Temkin model; that is, the activities of Cr_2O_3 and Fe_2O_3 will be equivalent to the square of their mole fractions. This is further supported by the facts that Fe_2O_3 and Cr_2O_3 have the same crystal structure, and that the cations are nearly the same size: Cr^{3+} (0.615 Å) and Fe^{3+} (0.645 Å), according to the Shannon and Prewitt scale [17] for six-fold coordination.

The activities of components in the spinel solid solution

When tie lines between two phases in equilibrium are known and activity data for one phase are available, the activities of the components in the second phase can be derived using the following modified Gibbs–Duhem integration method suggested by Wagner [18] and applied to oxide systems by Muan [16]. In the present calculation, $Ni_{0.5}FeO_2$, $Ni_{0.5}CrO_2$, $FeO_{1.5}$, and $CrO_{1.5}$ are used as the composition variables.

The intra-crystalline ion-exchange equilibrium is written as

$$FeO_{1.5} + Ni_{0.5}CrO_2 = Ni_{0.5}FeO_2 + CrO_{1.5} \tag{1}$$

The modified Gibbs–Duhem integration is given by

$$\log \gamma_{Ni_{0.5}FeO_2} = \int_1^{x_{Ni_{0.5}FeO_2}} x_{Ni_{0.5}CrO_2} \, d \log \left[\frac{a_{FeO_{1.5}}}{a_{CrO_{1.5}}}\right] \left(\frac{x_{Ni_{0.5}CrO_2}}{x_{Ni_{0.5}FeO_2}}\right) \tag{2}$$

The quantity in the bracket is obtained by assuming that the corundum solid solution obeys an ideal Temkin law as described above, while the quantity in parentheses is obtained from the results of this study.

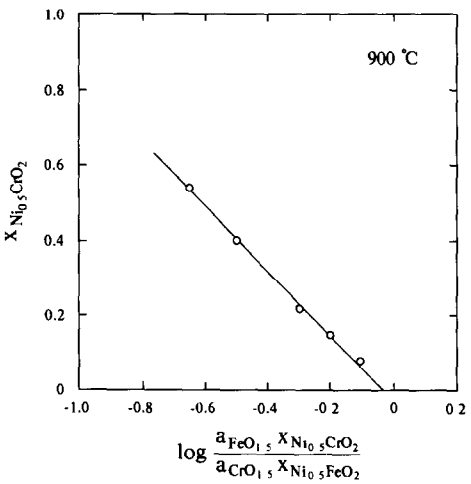

Fig. 2. Modified Gibbs–Duhem integration plot at 900°C.

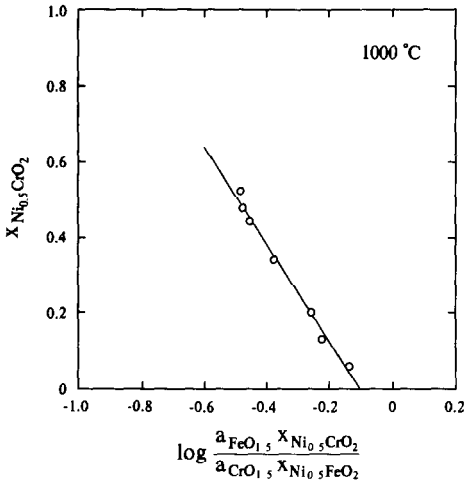

Fig. 3. Modified Gibbs–Duhem integration plot at 1000°C.

The modified Gibbs–Duhem integration plots for $Ni_{0.5}CrO_2$ and $Ni_{0.5}FeO_2$ are shown in Figs. 2 and 3. In these plots, mole fractions of $Ni_{0.5}CrO_2$ and $Ni_{0.5}FeO_2$ can be recalculated as $x_{Ni_{0.5}CrO_2} + x_{Ni_{0.5}FeO_2} = 1$. The value of log $\gamma_{Ni_{0.5}FeO_2}$ is obtained by the area below the curve in Figs. 2 and 3, while log $\gamma_{Ni_{0.5}CrO_2}$ can be evaluated from the area above the curve. However, there is considerable uncertainty in extrapolating curves of logarithmic terms versus $x_{Ni_{0.5}CrO_2}$ to $x_{Ni_{0.5}CrO_2} = 1$, owing to the lack of data for Fe_2O_3-poor compositions. For this reason, the activities of $Ni_{0.5}CrO_2$ were determined by Gibbs–Duhem integration plot. The results are shown in Fig. 4. It should be noted that the straight lines indicated in Figs. 2 and 3 suggest that the spinel solid solution is "regular". The regular

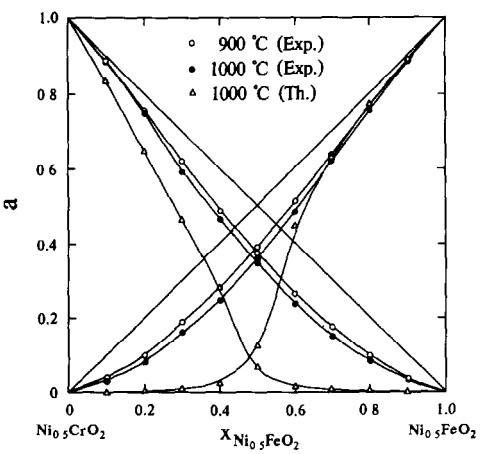

Fig. 4. Activities for $Ni_{0.5}FeO_2$ and $Ni_{0.5}CrO_2$ in spinel solid solution at 900 and 1000°C.

solution parameter α was determined either by the slope, which is equal to $(RT/2\alpha)$, or the area, which is equal to $\log \gamma_{Ni_{0.5}FeO_2} = \alpha x^2_{Ni_{0.5}CrO_2}/RT$. These values should be constant regardless of temperature, but those for α obtained at 900 and 1000°C are found to be -13.1 and -10.4 kJ mol^{-1}, respectively.

Comparison with the cation distribution model [2]

The distribution of cations between the tetrahedral and octahedral sites of pure spinels can be estimated from octahedral site preference energies, assuming ideal Temkin mixing of cations on each cation sub-lattice [1–4]. Jacob and Alcock [19] have shown that the cation distribution estimated from the site preference energies for a number of aluminate spinels is in good agreement with X-ray and neutron diffraction measurements. The approach used by Jacob and Alcock [2] is used to estimate the activity–composition relationship in the present intra-crystalline ion-exchange equilibria between tetrahedral and octahedral sites. The values for the octahedral site preference energies for Ni^{2+} (-86.2 kJ mol^{-1}), Fe^{3+} (0 kJ mol^{-1}) and Cr^{3+} (-157.7 kJ mol^{-1}) obtained by Dunitz and Orgel [20] from crystal-field theory are used.

The intra-crystalline exchange equilibria can be written, and the enthalpy change for the exchange equilibria ΔH^{EX} can be reduced from the site preference energies for $Ni_{0.5}CrO_2$

$$(Ni^{2+}) + [Cr^{3+}] = (Cr^{3+}) + [Ni^{2+}] \qquad \Delta H^{EX} = 71.5 \text{ kJ mol}^{-1} \tag{3}$$

and for $Ni_{0.5}FeO_2$

$$(Ni^{2+}) + [Fe^{3+}] = (Fe^{3+}) + [Ni^{2+}] \qquad \Delta H^{EX} = -86.2 \text{ kJ mol}^{-1} \tag{4}$$

where ( ) and [ ] denote tetrahedral and octahedral sites, respectively. The cation distribution on octahedral sites is calculated from the solution to the following pair of equations [2,21–23]

$$71.5 = -RT \ln\left[\frac{[x_{Ni^{2+}}]2\{x_{NiCr_2O_4} - [x_{Cr^{3+}}]\}}{\{1 - 2[x_{Ni^{2+}}]\}[x_{Cr^{3+}}]}\right] \tag{5}$$

$$-86.2 = -RT \ln\left[\frac{[x_{Ni^{2+}}]2\{x_{NiFe_2O_4} - [x_{Fe^{3+}}]\}}{\{1 - 2[x_{Ni^{2+}}]\}[x_{Fe^{3+}}]}\right] \tag{6}$$

where $[x_i]$ and x_i represent the ion fraction on the octahedral site and the mole fraction of each spinel component, respectively.

The calculated results for the cation distributions are listed in Table 2.

The activities can be evaluated from the cation distribution values relative to a normal spinel for $Ni_{0.5}CrO_2$, and relative to an inverse spinel

TABLE 2

Calculated cation distributions based on the cation distribution model

Composition	Tetrahedral site, number of ions			Octahedral site, number of ions		
$x_{Ni_{0.5}FeO_2}$	(Fe^{3+})	(Cr^{3+})	(Ni^{2+})	$[Fe^{3+}]$	$[Cr^{3+}]$	$[Ni^{2+}]$
0	0	4.655×10^{-2}	9.534×10^{-1}	0	1.953	0.046
0.1	0.200	7.943×10^{-3}	7.921×10^{-1}	1.526×10^{-5}	1.792	0.208
0.2	0.400	2.757×10^{-3}	5.973×10^{-1}	7.837×10^{-5}	1.597	0.403
0.3	0.600	1.081×10^{-3}	3.992×10^{-1}	2.624×10^{-4}	1.399	0.601
0.4	0.799	3.502×10^{-4}	2.006×10^{-1}	9.258×10^{-4}	1.200	0.799
0.5	0.983	1.979×10^{-5}	1.675×10^{-2}	1.677×10^{-2}	1.000	0.983
0.6	0.999	1.311×10^{-6}	1.439×10^{-3}	2.014×10^{-1}	0.800	0.999
0.7	0.999	4.172×10^{-7}	7.243×10^{-4}	4.007×10^{-1}	0.600	0.999
0.8	0.999	2.086×10^{-8}	4.836×10^{-4}	6.005×10^{-1}	0.400	1.000
0.9	1.000	8.941×10^{-9}	3.629×10^{-4}	8.004×10^{-1}	0.200	1.000
1.0	1.000	0	2.904×10^{-4}	1.000	0	1.000

for $Ni_{0.5}FeO_2$, as the standard state, using the equations [10]

$$a_{Ni_{0.5}CrO_2} = \frac{[x_{Cr^{3+}}](x_{Ni^{2+}})^{1/2}}{[x_{Cr^{3+}}]_o(x_{Ni^{2+}})_o^{1/2}} \tag{7}$$

$$a_{Ni_{0.5}FeO_2} = \left[\frac{[x_{Fe^{3+}}](x_{Fe^{3+}})[x_{Ni^{2+}}]}{[x_{Fe^{3+}}]_o(x_{Fe^{3+}})_o[x_{Ni^{2+}}]_o}\right]^{1/2} \tag{8}$$

where $(\,)_o$ and $[\,]_o$ denote ion fractions in pure components.

The calculated results for activities of spinel components and for Gibbs energy of mixing ΔG^M are given in Figs. 4 and 5, which indicate that the experimental values for ΔG^M are less negative than those of the model. The values for Gibbs energy of mixing in other spinel solid solutions with common cations, obtained by Jacob and co-workers [11,21–23], are included in Fig. 5 for comparison, along with that obtained at 1000°C according to Temkin's law. It is of interest to note that the values for ΔG^M in the group of normal–normal spinel solid solutions are approximately half the values in the group of normal–inverse spinel solid solutions, except for the $Fe_{0.5}AlO_2$–$Fe_{1.5}O_2$ system.

It has been shown that the correlation between experimentally derived and calculated Gibbs energy of mixing values is very poor in most spinel solid solutions. Therefore, Jacob and co-workers [11,23] discussed the difference between theoretical and experimental values ($\Delta G^M_{th} - \Delta G^M_{exp}$) in terms of the lattice distortion effect due to cation size difference.

The present results are shown in Fig. 6, with those obtained in other spinel solid solutions [11,21–23] with common cations. It can be seen that, in the normal–inverse spinel solid solutions, these values increase in the order $Ni_{0.5}CrO_2$–$Ni_{0.5}FeO_2$ > $Fe_{0.5}AlO_2$–$Fe_{1.5}O_2$ > $Fe_{0.5}CrO_2$–$Fe_{1.5}O_2$,

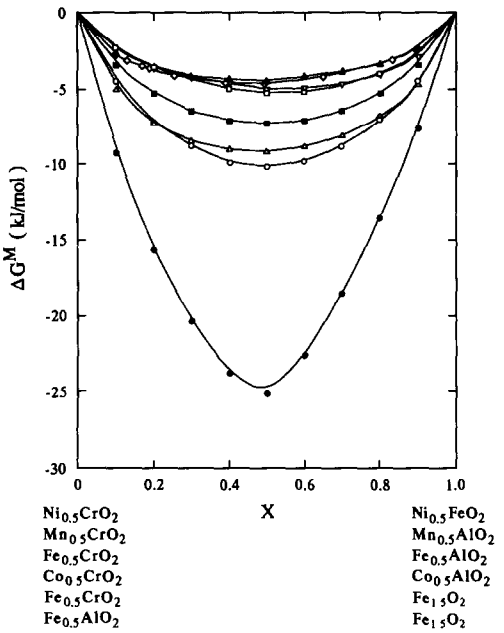

Fig. 5. Gibbs energy of mixing of $Ni_{0.5}FeO_2$–$Ni_{0.5}CrO_2$ at 1000°C for the various spinel solution systems: ○, $Ni_{0.5}CrO_2$–$Ni_{0.5}FeO_2$ (experimental); ●, $Ni_{0.5}CrO_2$–$Ni_{0.5}FeO_2$ (theoretical); ■, Temkin solution (1000°C); ▲, $Mn_{0.5}CrO_2$–$Mn_{0.5}AlO_2$ [23]; ◇, $Fe_{0.5}CrO_2$–$Fe_{0.5}AlO_2$ [22]; ▽, $Co_{0.5}CrO_2$–$Co_{0.5}AlO_2$ [23]; □, $Fe_{0.5}AlO_2$–$Fe_{1.5}O_2$ [21]; △, $Fe_{0.5}CrO_2$–$Fe_{1.5}O_2$ [11].

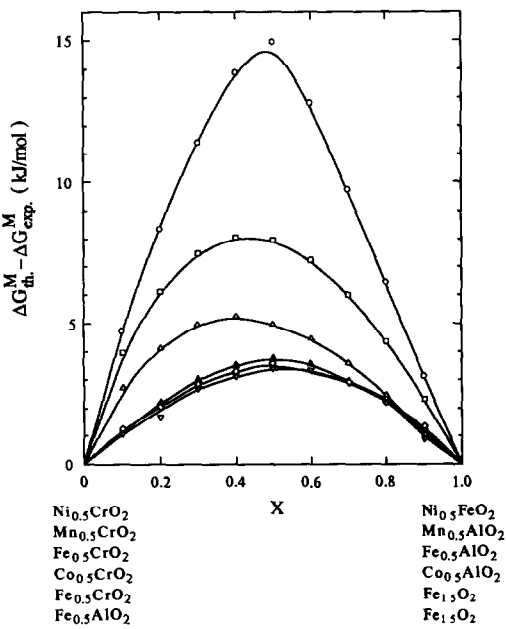

Fig. 6. Difference in Gibbs energy of mixing between theoretical and experimental values. (Symbols have same meaning as those in Fig. 5.)

which cannot be explained by the cation size difference, whereas in the normal–normal spinel solid solutions, the values are approximately the same. It must be noted, however, that the cation distribution model proposed by O'Neill and Navrotsky [4], in which the enthalpy of cation disordering ΔH^{EX} is not independent of the cation distribution in the spinel, seems to be more applicable to the thermodynamic properties of spinel solid solutions. This model was not applied to the present data, because the present spinel solid solution has a significant width of the spinel field, and the parameters for this model were not accurately determined.

CONCLUSIONS

The activities for $Ni_{0.5}FeO_2$ and $Ni_{0.5}CrO_2$ spinel solid solutions were determined from the experimental tie-line data at 900 and 1000°C, resulting in a regular solution with a negative deviation from ideality. The Gibbs energy of mixing in this system was found to be considerably less negative than that derived from the cation distribution model based on site preference energies. The observed values for ΔG^M were found to be approximately twice those observed in the normal–normal spinel solid solutions. The difference between the experimental and theoretical Gibbs energy of mixing values in the present system was greater than those observed in the previous spinel solid solutions.

REFERENCES

1 A. Navrotsky and O.J. Kleppa, J. Inorg. Nucl. Chem., 29 (1967) 2701.
2 K.T. Jacob and C.B. Alcock, J. Solid State Chem., 20 (1977) 70.
3 H. St.C. O'Neill and A. Navrotsky, Am. Mineral., 68 (1983) 181.
4 H.St.C. O'Neill and A. Navrotsky, Am. Mineral., 69 (1984) 733.
5 B.-H. Park and H. Suito, Iron Steel Int. J., 30 (1990) 426.
6 H. Todoroki and H. Suito, Scand. J. Metall., 20 (1991) 211.
7 A.E. Paladino, Jr., J. Am. Ceram. Soc., 42 (1959) 168.
8 M.W. Shafer, J. Phys. Chem., 65 (1961) 2055.
9 H.M. O'Bryan, F.R. Monforte and R. Blair, J. Am. Ceram. Soc., 48 (1965) 577.
10 A.D. Pelton, H. Schmalzried and J. Sticher, J. Phys. Chem. Solids, 40 (1979) 1103.
11 A. Petric and K.T. Jacob, J. Am. Ceram. Soc., 65 (1982) 117.
12 V. Cremer, Neues Jahrb. Mineral. Abh., 111 (1969) 184.
13 R. Snethlage and D. Klemm, Neues Jahrb. Mineral. Abh., 125 (1975) 227.
14 N.G. Schmahl and H. Dillenburg, Z. Phys. Chem. N.F., 65 (1969) 119.
15 T. Katsura, M. Nakihara, S-I. Hara and T. Sugihara, J. Solid State Chem., 13 (1975) 107.
16 A. Muan, Proc. Br. Ceram. Soc., 8 (1967) 103.
17 R.D. Shannon and C.T. Prewitt, Acta Crystallogr. Sect. B, 25 (1969) 925.
18 C. Wagner, Thermodynamics of Alloys, Addison-Wesley, Reading, MA, 1955.
19 K.T. Jacob and C.B. Alcock, Met. Trans., 6B (1975) 215.
20 J.D. Dunitz and L.E. Orgel, J. Phys. Chem. Solids, 3 (1957) 318.
21 A. Petric, K.T. Jacob and C.B. Alcock, J. Am. Ceram. Soc., 64 (1981) 632.
22 A. Petric and K.T. Jacob, Solid State Ionics, 6 (1982) 47.
23 K.T. Jacob, G.N.K. Iyengar and W.K. Kim, J. Am. Ceram. Soc., 69 (1986) 487.